



**Nanoparticles decorated coal tar pitch based carbon foam
with enhanced electromagnetic radiation absorption
capability**

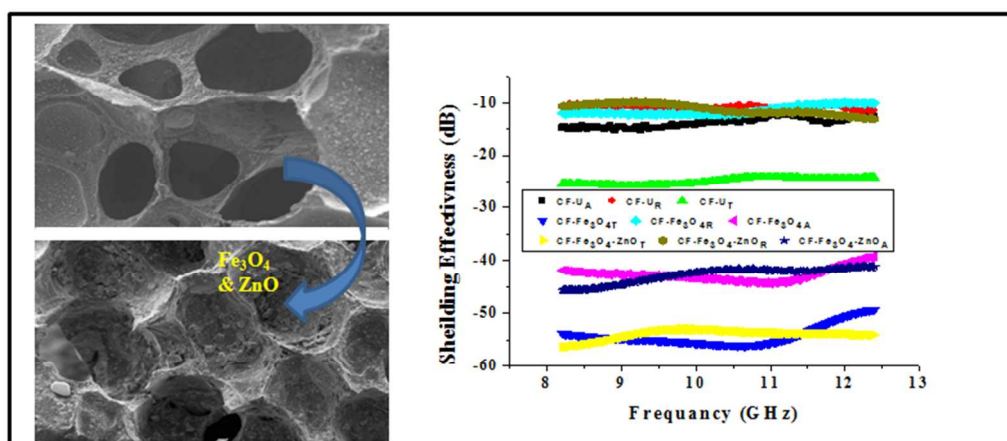
Journal:	<i>RSC Advances</i>
Manuscript ID:	RA-ART-01-2015-000247.R1
Article Type:	Paper
Date Submitted by the Author:	21-Jan-2015
Complete List of Authors:	Kumar, Rajeev; CSIR-NPL, Gupta, Ashish; CSIR-NPL, Dhakate, Sanjay; CSIR-National Physical Laboratory, New Delhi, Physics & Engineering of Carbon

Nanoparticles decorated coal tar pitch based carbon foam with enhanced electromagnetic radiation absorption capability

Rajeev Kumar, Ashish Gupta and Sanjay R. Dhakate*

Physics and Engineering of Carbon, Division of Materials Physics and Engineering,
CSIR-National Physical Laboratory, Dr. K. S. Krishnan Marg, New Delhi-110012 (India)

Carbon foam decorated with magnetic and dielectric nanoparticle are significantly improved the EM radiation absorption in the X-band frequency region.



Nanoparticles decorated coal tar pitch based carbon foam with enhanced electromagnetic radiation absorption capability

Rajeev Kumar, Ashish Gupta and Sanjay R. Dhakate*

Physics and Engineering of Carbon, Division of Materials Physics and Engineering,
CSIR-National Physical Laboratory, Dr. K. S. Krishnan Marg, New Delhi-110012 (India)

Abstract

In the present study, to replace existing high density radar absorbing materials (RAM) for civil and military aerospace applications, light weight coal tar pitch based carbon foam (CFoam) was developed by sacrificial template technique. The CFoam was decorated with Fe_3O_4 and ZnO nanoparticles to improve electromagnetic (EM) radiation absorption in to make them useful as RAM. To ascertain the effect of decorated nanoparticles on the CFoam, it was characterized by Scanning electron microscopy, X-ray diffraction, vector network analyzer and vibration sample magnetometer. It was observed that, Fe_3O_4 and Fe_3O_4 -ZnO nanoparticles have positive effect on the overall properties of CFoam. The compressive strength of CFoam increases by 22 % and thermal stability by 100°C whereaselectrical conductivity decreases almost by 25%. The total shielding effectiveness (SE) of CFoam increases from -25 dB to -54 and -56 dB of Fe_3O_4 and Fe_3O_4 -ZnO nanoparticles decorated CFoam. The enhancement in total SE of Fe_3O_4 and Fe_3O_4 -ZnO coated CFoam is basically due to the contribution of absorption losses by -42 and -45 dB. The Fe_3O_4 and Fe_3O_4 -ZnO coating increases surface resistance and magnetic properties. Because the ferromagnetic nanoparticles act as tiny dipoles which get polarized in the presence of EM field and result in better absorption of EM radiation. This clearly demonstrates that decorated nanoparticles in conducting light weight CFoam is useful as RAM for different applications to attenuate EM radiation.

Key words: Carbon Foam; Scanning electron microscopy (SEM); Electrical conductivity; Magnetic properties, Electromagnetic shielding effectiveness.

*Corresponding author. Tel: 0911145608257. E-mail: dhakate@mail.nplindia.org (S.R. Dhakate)

1. Introduction

In the modern technological world, scientists are constantly in the search of new materials to replace existing high density radar absorbing materials (RAM) for civil and military aerospace applications. In these applications it is usually important for aircraft and ships to suppress microwave reflection so as to improve their combat survivability. The absorption of the electromagnetic energy in medium between the radar and a protected target by use of RAM is one approach to reduce the radar signatures of targets¹. RAM is classified into two categories as magnetic and dielectric absorbing materials. The magnetic absorbers depend on the magnetic hysteresis effect, which is attained in magnetic materials such as ferrites. But densities of the magnetic materials are generally high and absorbing bandwidths for magnetic absorbers are usually narrow. On the other hand, dielectric materials are light weight but do not match up to the absorptivity of magnetic absorbers²⁻⁴. These two types of materials have different advantages and disadvantages when they are applied as absorbers. They can be used together as a composite, and the magnetic material is usually the base one, but high density of the material is still of great concern. Therefore, in order to meet desired requirements, many materials have been singled out or synthesized, among them carbon materials have been considered as the most promising candidates since World War II⁵. Carbon based materials are available naturally or synthesized from organic and inorganic precursor. The physical, mechanical, electrical and thermal properties of carbon material can be tailored by controlling processing parameters. Generally, technologists and scientists are looking for highly efficient, thermally conducting and lightweight EMI shielding material, particularly for aerospace transportation vehicles and space structural application. Among the different carbon materials, light weight carbon foam (CFoam) has emerged as a promising candidate for EMI shielding owing to its outstanding properties such as low density, large surface area with open cell wall structure, good thermal/electrical transport properties and mechanical stability^{6, 7}. Light weight CFoam is a sponge-like, rigid and high performance engineering material in which carbon ligaments are interconnected to each other. In early days CFoam is prepared from thermosetting polymeric material by heat treatment under controlled atmosphere⁸. Later on, coal tar and petroleum pitches are used for CFoam synthesis⁹. The foam derived from organic polymer and pitches gives low thermal conductivity, and these are predominantly used as a thermal insulating material¹⁰⁻¹⁴. To develop crystalline CFoam of high electrical and thermal conductivity, it generally prepared from mesophase pitch by high

temperature and high pressure foaming technique^{15, 16}. It is an expensive process, therefore in the present study, using the simple sacrificial template¹⁷ technique CFoam is developed from the modified coal tar pitch¹⁸. In the electrically conductive CFoam, electromagnetic (EM) shielding effectiveness(SE) is dominated by reflection losses rather than absorption^{19, 20}. Therefore, to improve microwave absorption in CFoam, it heat treated at lower temperature so that it will be dielectric or low electrical conductivity. But to use the CFoam as RAM in civil and military aerospace applications, it required material should be thermally stable and conductive so that heat generated due to the absorption of electromagnetic radiations cannot be damage electronic components in the system as well. However, the CFoam processing carried out at low temperature does not give adequate thermal stability and conductivity.

Therefore, it required to coat or decorates CFoam with magnetic/dielectric nanomaterials, so that CFoam can acts as excellent microwave absorbing material with requisite thermal stability and conductivity. In which microwave can be absorbed is due to the different interactive energy dissipation processes of polarization and magnetization²¹. In this direction, in the present investigation coal tar pitch derived CFoams are developed by sacrificial template technique and heat treated to 1000°C in inert atmosphere. These foams are coated by ferromagnetic ferrofluid and dielectric zinc oxide (ZnO) nanoparticles to improve the radar emission absorption. The ferrofluid is a suspension Fe₃O₄ nanoparticle in organic solvent. The nanosize Fe₃O₄ is a kind of magnetic functional nanomaterial, which has been widely used as microwave radiation absorbers^{22, 23}. To ascertain effect of Fe₃O₄ and ZnO coating on CFoam, coated and uncoated CFoams are characterized by Scanning electron microscopy, X-ray diffraction, vector network analyzer and vibration sample magnetometer, for compressive strength and electrical conductivity.

2. Experimental

2.1 Development of carbon foam

The CFoam was developed by sacrificial template technique from modified coal tar pitch. The starting coal tar pitch possess softening point 86.6°C, quinoline insoluble (QI) 0.2%, toluene insoluble (TI) 15.9 % and coking value 47.6%. The coal tar pitch was modified by heat treating at 400°C for 5 hours. The modified coal tar pitch possess softening point 236°C, QI content 23.6 %, TI content 63.0% and coking value 78.5% respectively. The water slurry of modified

coal tar pitch with 3% polyvinyl alcohol (PVA) was impregnated into a polyurethane foam (procured from S. G. & Company, New Delhi with density 0.030 g/cc and average pore size 0.45 mm) template under vacuum. The modified coal tar pitch impregnated polyurethane foam was converted into CFoam by several heat treatments in air as well as in an inert atmosphere up to 1000°C²⁴. Initially, the modified coal tar pitch impregnated foams were heat treated @1°C/min up to 275°C in the nitrogen atmosphere for 1 h followed by oxidation and stabilization in air atmosphere at temperature 300°C. The stabilized foam was carbonized in tubular high temperature furnace at 1000°C with heating rate 10°C/hr in inert atmosphere.

Fe₃O₄ nanoparticles were synthesized by well-established chemical co-precipitation method^{25, 26}. The solution containing ferric (Fe³⁺) chloride and ferrous (Fe²⁺) sulfate was introduced in deionized water. The mixture was stirred for an hour and oleic acid was added as a surfactant. The addition of base (20-25 ml ammonia solution) was carried out at 80°C by maintaining the pH 9-10. Nanoparticles were magnetically decanted and washed several times with deionized water to remove unwanted residual of salt. To obtain ferrofluid, this wet slurry was dispersed in kerosene and centrifuged. The ZnO nanoparticles are prepared by thermal evaporation of zinc acetate²⁷ at 60-70°C at slow heating. The CFoam was coated with ferrofluid solution and another case with ferrofluid-zinc oxide solution by weight of 0.5: 0.5 ratios. After coating of ferrofluid and ferrofluid-zinc oxide nanoparticles, these CFoams were heat treated at 650°C for 10 minute in inert atmosphere. The process for synthesis of as such CFoam, Fe₃O₄ and Fe₃O₄-ZnO coated CFoam is shown in figure 1. The CFoam uncoated and coated were designated as uncoated CFoam (CF-U), Fe₃O₄ coated CFoam as (CF-Fe₃O₄) and Fe₃O₄-ZnO coated CFoam as (CF- Fe₃O₄-ZnO).

2.2. Characterization

The weight percentage of nanoparticles in CFoam was evaluated by thermo gravimetric analyzer (TGA, Mettler Toledo), the nanoparticle decorated CFoam heated up to 1000°C in air atmosphere and during heat treatment carbon will be oxidizing completely and residue remain at the end of heat treatment is in the form of nanoparticles. The bulk density of foam was measured by ASTM standard (ASTM C559), bulk density was a ratio of weight of the CFoam in air and volume. The weight of the CFoam was measured by digital balance (model ME40290) and volume of CFoam by measuring the dimensions with the help of digital vernier calipers. The

compressive strength of all CFoam was measured on universal INSTRON testing machine model 4411 as per ASTM standard. The thermal conductivity of CFoam was measured by laser flash method having xenon laser as a source in thermo flash line 2003 instrument (Anter Corporation, USA). By laser flash method, thermal diffusivity and specific heat of each sample was measured at 25°C. The thermal conductivity then calculated from the equation, $\alpha = k / (\rho \cdot Cp)$, where α is the thermal diffusivity, k is thermal conductivity, Cp is the specific heat and ρ is density of the foam.

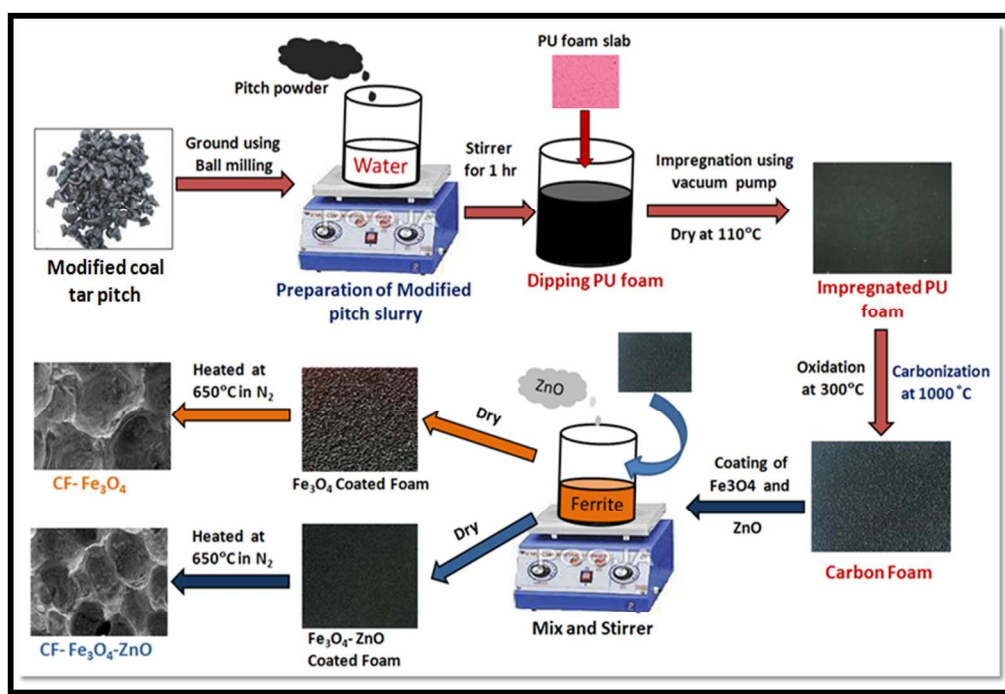


Figure 1: Process for synthesis of as such CFoam, Fe₃O₄ and Fe₃O₄-ZnO coated CFoam.

Raman spectra of the CFoam samples were recorded using Renishaw inVia Raman spectrometer, UK with laser as an excitation source at 514 nm. The crystal structure of CFoams were studied by X-ray diffraction (XRD, D-8 Advanced Bruker diffractometer) using CuK α radiation ($\lambda = 1.5418 \text{ \AA}$). The surface morphology of the samples was observed by scanning electron microscope (SEM, Leo model, S-440). The electrical conductivity CFoam was measured by d.c. four probe contact method using a Keithley 224 programmable current source for providing current. The voltage drop was measured by Keithley 197A auto ranging digital micro voltmeter. The values reported in text are averaged over six readings of voltage drops at

different portions of the sample. Electromagnetic interference shielding effectiveness (EMI-SE) was measured by waveguide using vector network analyzer (VNA E8263B, Agilent Technologies). The rectangular samples of thickness 2.75 mm were placed inside the cavity of sample holder which matches the internal dimensions of X-band (8.4-12.4 GHz) wave guide. The sample holder was placed between the flanges of the waveguide connected between the two ports of VNA. A full two port calibration was performed using quarter wavelength offset and terminations and keeping input power level at -5.0 dBm. The magnetic property of the foam samples were measured by vibration sample magnetometer (VSM) model 7304, Lakeshore Cryotronics Inc., USA with a maximum magnetic field of 1.2T, vibrating horizontally at frequency 76 Hz. Thermal stability of the CFoam is investigated by TGA in air atmosphere @ 10°C/min.

3. Results and Discussion

The physical and mechanical properties of CFoam are reported in Table 1. The bulk density of CF-U heat treated at 1000°C is 0.55 g/cc and that of Fe₃O₄ and Fe₃O₄-ZnO nanoparticles coated CFoams (CF-Fe₃O₄ and CF-Fe₃O₄-ZnO) bulk density increases to 0.58 g/cc. The thin coatings of nanoparticles help increasing in bulk density of CFoam by more than 10 %. Improvement in the bulk density has positive effect on the mechanical properties of CFoam.

The nanoparticles are embedded by weight percentage in both the cases, in Fe₃O₄ embedded foam, nanoparticles content is 9 weight % and in Fe₃O₄ -ZnO embedded foam nanoparticles content is 10.weight % is confirmed by TGA. Since the density of Fe₃O₄ and ZnO nanoparticles is 4.8 and 5.6 g/cc, therefore enhancement in the density almost is same (by 11.5 % increase in the density) of nanoparticles embedded carbon foam.

The compressive strength of CF-U is 7.50 MPa and that of CF-Fe₃O₄ is 8.90 MPa. While in case of foam CF-Fe₃O₄-ZnO, compressive strength increases from 7.50 MPa to 9.20 MPa. Hence, there is an increase of 22 % compressive strength of Fe₃O₄ and Fe₃O₄-ZnO nanoparticles embedded CFoams. The improvement in compressive strength of Fe₃O₄ and Fe₃O₄-ZnO nanoparticles embedded CFoam is due to the higher value compressive strength of nanoparticles as well as increases in density of foam and a result as a high value of nanoparticle density (Fe₃O₄ and ZnO nanoparticles is 4.8 and 5.6 g/cc). On the other hand, the compressive strength of CFoam also depends upon microstructure. The microstructure mainly includes width of the

ligaments and quantity of microcracks. In case of CF-U, load is transferred through ligaments; therefore, cracks in the ligaments can be responsible for low load bearing capacity of CFoam. While in case of Fe₃O₄ and Fe₃O₄-ZnO coated CFoam, Fe₃O₄ and ZnO nanoparticles are infiltrated in the cracks, deposited on the ligaments, inside and on the surface of pores, this resulted in to increase in bulk density and reduced the cracks density. Thus, in case of CF-Fe₃O₄ and CF-Fe₃O₄-ZnO, nanoparticles are infiltrated in the cracks, deposited on the ligaments which can help in deflecting and carrying applied load. This attributes to the improvement in the compressive strength of CFoams.

Table 1: Properties of CFoam

Properties	CF-U	CF-Fe ₃ O ₄	CF-Fe ₃ O ₄ -ZnO
Bulk density (gcm ⁻³)	0.52	0.58	0.58
Compressive strength (MPa)	7.5	8.9	9.2
Electrical conductivity (Scm ⁻¹)	55.0	42.0	40.0
Thermal conductivity (Wm ⁻¹ K ⁻¹)	20.0	-	-

The nanoparticles will affect the conductivity of the CFoam because the conductivity of Fe₃O₄ and ZnO nanoparticles are comparatively less than CFoam heat treated at 1000°C. The electrical conductivity of CFoam CF-U is 55 S.cm⁻¹ due to the delocalized π electron in the carbon network in the coal tar pitch derived CFoam. However, in case of Fe₃O₄ coated foam (CF-Fe₃O₄), electrical conductivity decreases to 42 S.cm⁻¹ and in Fe₃O₄-ZnO coated foam the electrical conductivity is almost same with the conductivity of CF-Fe₃O₄-ZnO. The decrease in conductivity is due to the Fe₃O₄ and ZnO inhibit in the conduction path of electrons. Also the Fe₃O₄ and ZnO coated mostly on the surface and infiltrated in the open pores and as a consequence surface resistant increases of CFoam. The conduction path decreases due to the interactions of magnetic and dielectric material with carbon during heat treatment at above 600°C. The thermal conductivity is also one of the important criteria for quick heat dissipation in CFoam used in civil and military aerospace vehicles to protect them from thermal heating of

electronic power systems. The thermal conductivity of a material is governed by lattice vibrations. The thermal conductivity of CFoam (CF-U) is in the range of 20 W/m.K and which is influenced by structure of the foam in which most of the heat is transfer by the ligaments and cell wall. In **Figure 2 (a-c)** illustrated SEM images of CFoam. In case of CF-U (Figure 2 (a)), cells are not of exactly spherical in size and distributions of cells are not uniform. The cell geometry significantly influence by the morphology of template foam. All the cells are not open and some of them are incomplete cell membrane and each cell is sealed off from its neighbors partly i.e., ligaments. While in CF-Fe₃O₄ (Figure 2 (b)), Fe₃O₄ particles are coated on the ligaments and infiltrated in the pores and some of the nanoparticles are agglomerated, this resulted in to bigger particles. The size of Fe₃O₄ nanoparticles (10-15 nm) is shown in Figure 3 (a). In case of CF-Fe₃O₄-ZnO (Figure 2 (c)), both types of nanoparticles coated on ligaments and infiltrated inside the pores but the extent of agglomeration is less as compared to CF-Fe₃O₄. It is interesting to note that the bigger particle size of ZnO (**Figure 3 (b)**) restrict the agglomeration of Fe₃O₄ in case of CF-Fe₃O₄-ZnO.

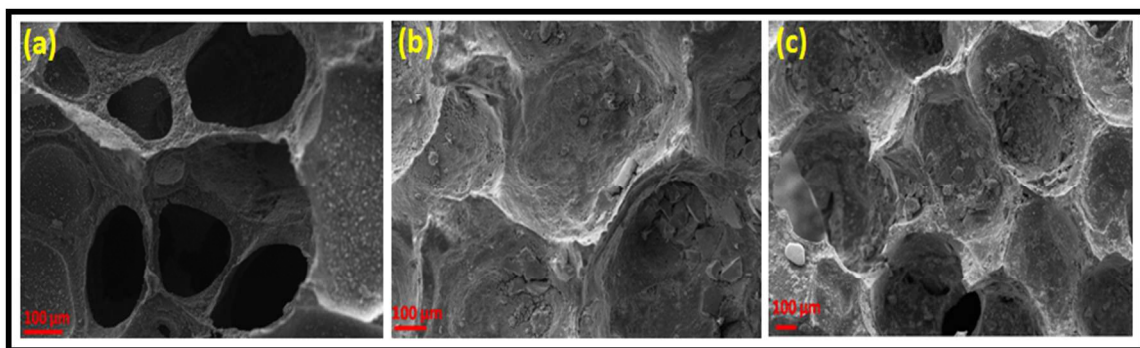


Figure 2: SEM micrographs of CFoam (a) CFU, (b) CF-Fe₃O₄ and (c) CF-Fe₃O₄-ZnO

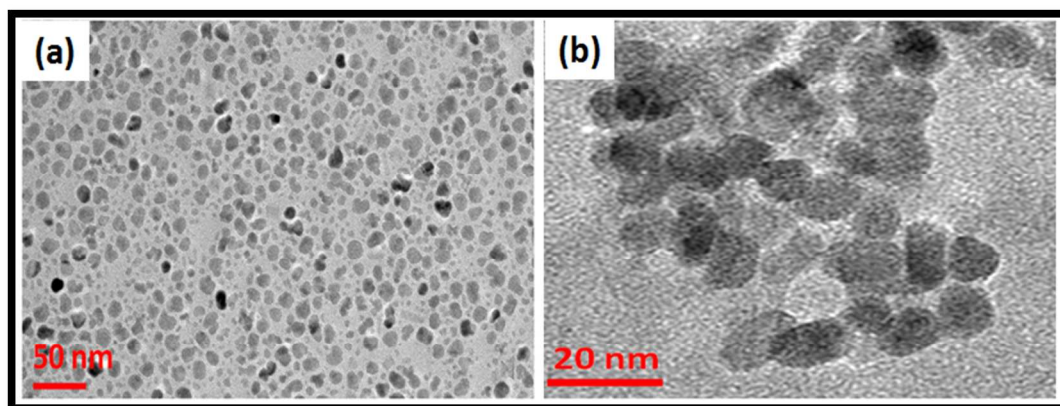


Figure 3: TEM micrograph (a) Fe₃O₄ and (b) ZnO

Figure 4 (a-d) shows the XRD curve of CFU, Fe₃O₄ and ZnO nanoparticles, CF-Fe₃O₄ and CF-Fe₃O₄-ZnO. In case of CFU (figure 4 (a)), carbon derived from graphitized coal tar pitch consist of three peaks at $2\theta = 24.98, 43.44$ and 79° are correspond to the carbon of 002, 101 and 110 lattice plan. Broad peak (002) interlayer spacing (d spacing) corresponds to $d_{002} = 0.3566$ nm indicating carbonized disorder carbon. The XRD pattern of the Fe₃O₄ nanoparticles (figure 4 (b)) shows quite identical to pure magnetite and matched well with JCPDS No.19-0629, this

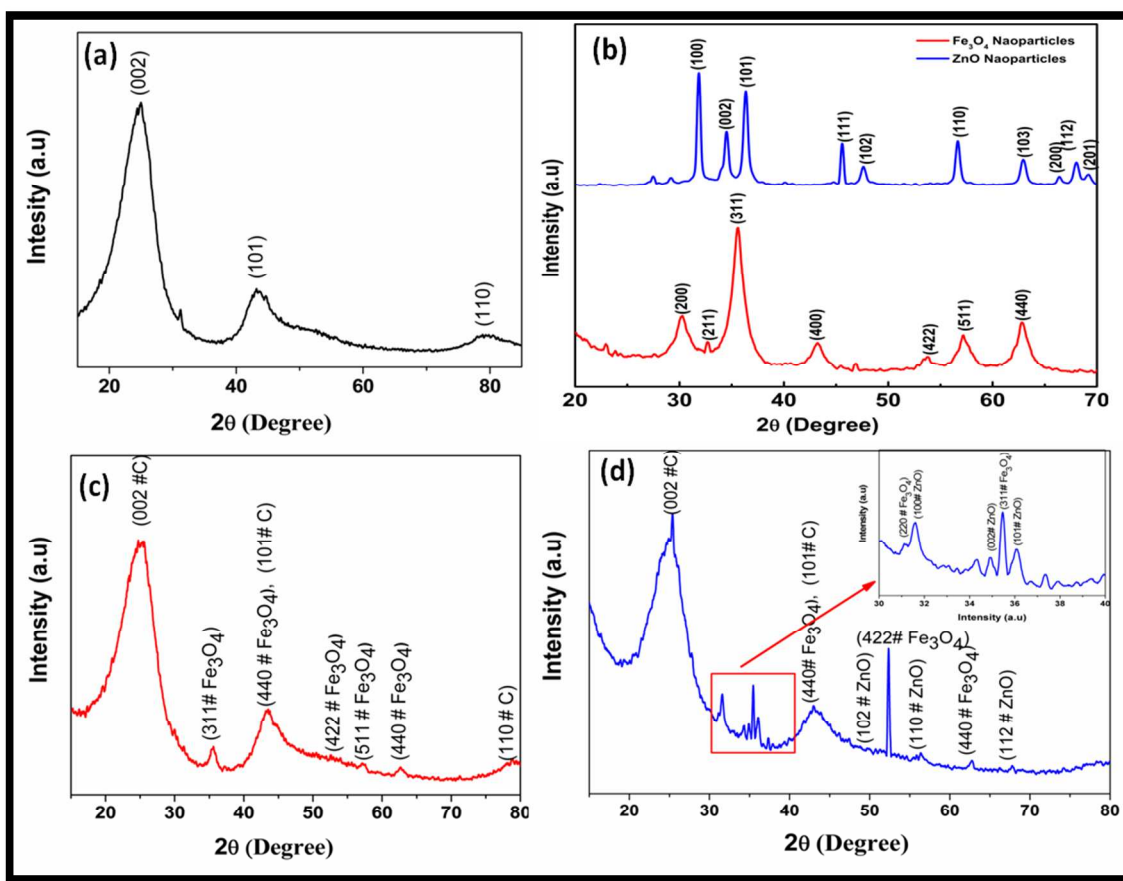


Figure 4: XRD spectra of CFoam (a) CFU, (b) Fe₃O₄ and ZnO nanoparticles (c) CF-Fe₃O₄ and (d) CF-Fe₃O₄-ZnO

indicates that the sample has a cubic crystal system²⁸. The mean crystallite size (10.5 nm) is calculated from the XRD curve according to the line width of the (311) plane refraction peak using Scherrer equation. Also Figure 4 (b) shows the XRD pattern of the ZnO nanoparticles. The peaks at 2θ values $32.1, 34.7, 36.6, 47.9, 56.9, 63.2, 66.7, 68.3$ and 69.4° are equivalent to (100), (002), (101), (102), (110), (103), (200), (112) and (201) are confirm by JCPDS No 36-1451²⁹.

The results reveals that the ZnO nanoparticles are of wurtzite hexagonal type structure³⁰. Figure 4 (c) shows the XRD curve of CF-Fe₃O₄, it consist of peaks of carbon and Fe₃O₄ at 2θ equal to 25.22°, 35.1°, 43.26°, 44.6°, 53.72°, 57.15° and 62.55° and 78.92°. During the heat treatment, interactions between the carbon and Fe₃O₄ nanoparticles occur at temperature between 500-650°C, which form Fe-C (peak at 43.26).

It is well known that carbon is a reducing agent, which can react with Fe-O compounds during heat treatment and compounds Fe-O transform into iron carbide³¹. Also the peaks of Fe₃O₄ are shifted to lower diffraction angle, this suggest that successful incorporation of dopant in the host matrix. While in case of CF-Fe₃O₄-ZnO (figure 4(d)), it is observed that ZnO and Fe₃O₄ are coexisting with carbon, which results into the change in the peak position that has positive effect on the magnetic and dielectric properties of the CFoam. Therefore, CF-Fe₃O₄-ZnO consists of peaks amorphous carbon, Fe₃O₄ and ZnO at 2θ equal to 25.27, 31.3, 35.27, 35.7, 36.12, 42.99, 52.3, 56.4, 62.7 and 67.32° while some of ZnO peaks are relatively at lower intensity compared to carbon and Fe₃O₄ therefore, magnified view (XRD) of CF- Fe₃O₄-ZnO at 30-40° is show in inset figure of figure 4 (d).

Figure 5 shows the shielding effectiveness (SE) of CFU, CF-Fe₃O₄and CF-Fe₃O₄-ZnO in the frequency range 8.2 to 12.4 GHz. It is well known that the properties of CFoam can influence by its processing temperature because structure of carbon materials modified with increasing processing heat treatment temperature³². As a consequence increase in electrical conductivity of carbon material with increasing processing temperature. In this investigation CFoam used are heat treated to temperature 1000°C which have quite high value of electrical conductivity. Generally, electromagnetic (EM) radiations are reflecting from conducting material. The extent of reflection is depending on the electrical conductivity and morphology of shield material. While EM radiation absorption controlled by shield materials magnetic and dielectric properties.

The validation of CFoam as RAM or EM shield can be elucidating by the measuring SE in terms of reflection and absorption losses. The SE of a shield material is the ability to attenuate EM radiation that can be expressed in terms of ratio of incoming (incident) and outgoing (transmitted) power³³. The higher values of SE in decibels (dB) signify less energy passes through the shield and most of the energy absorb or reflected by shield material. The EM attenuation offered by shield or RAM may depend on the three mechanisms: reflection of the

wave from the front face of shield, absorption of the wave as it passes through the shield and multiple reflections of the waves at various interfaces³⁴. Therefore, total SE (SE_T) of RAM is attributed to three types losses viz. reflection loss (SE_R), absorption loss (SE_A) and multiple reflection losses (SE_M) and it can be expressed as,

$$SE_T(\text{dB}) = SE_R + SE_A + SE_M = 10 \log (P_t/P_i)$$

Where, P_i and P_t are power of incident and transmitted EM waves respectively. As, the P_t is always less than P_i , therefore, SE_T is a negative quantity and more negative value means increase in magnitude of SE. It is significant to note that the losses associated with multiple reflections can be ignored ($SE_M \sim 0$) when SE of EMI shielding material is more than -10 dB²⁰ so that SE can be expressed as, $SE_T(\text{dB}) = SE_R + SE_A$.

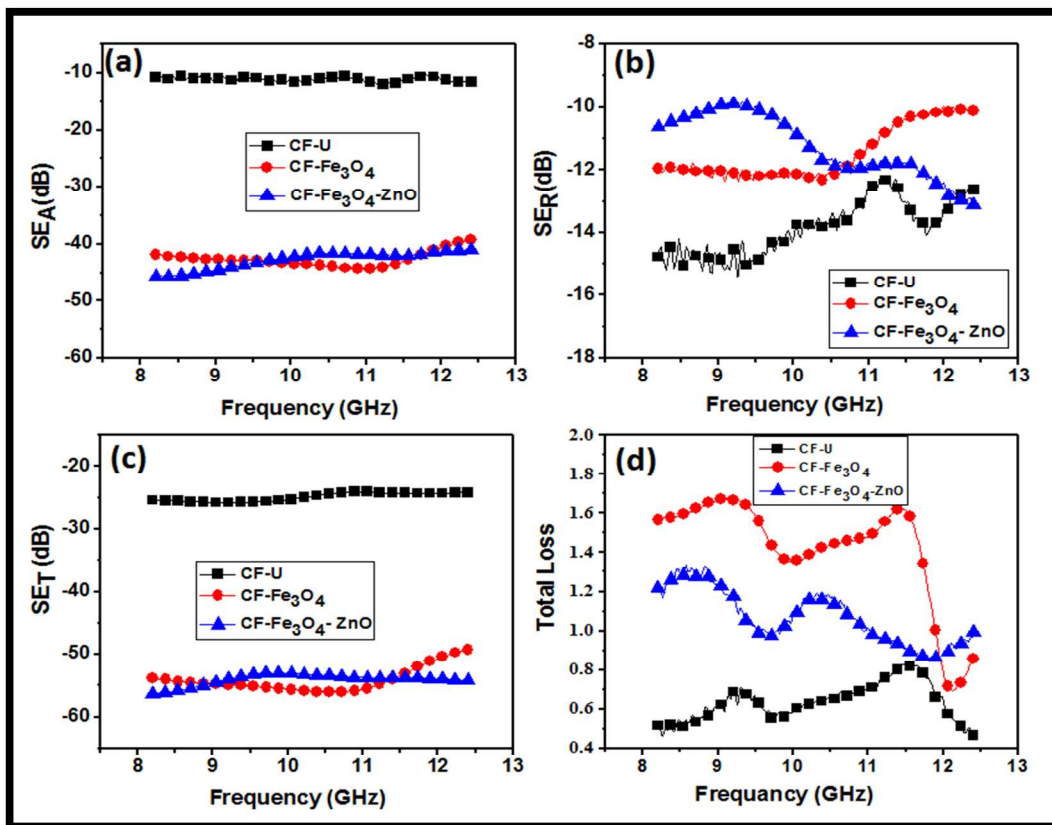


Figure 5: Shielding effectiveness of CFoam in 8.2 to 12.4 GHz (a) SE_A (b) SE_R (c) SE_T and (d) Total loss with increasing the frequency

Figure 5 show the SE_A , SE_R , and SE_T of CFoams in X-band frequency region. It is observed that SE_A is almost constant with increasing frequency (Figure 5 (a)). While SE_R varies with

frequency (Figure 5 (b)) and from figure 5 (c), it reveals that total SE is following the path of SE_A . The value of SE_T for CF-U is -25 dB while in case CF- Fe_3O_4 and CF- Fe_3O_4 -ZnO, it increases to -54 and -56dB. It is interesting to note that SE_T of CF- Fe_3O_4 and CF- Fe_3O_4 -ZnO twice than that of CF-U. In case of CF-U, SE_R (-14dB) is slightly higher than SE_A (-11 dB). On the other hand, SE_T in CF- Fe_3O_4 and CF- Fe_3O_4 -ZnO is governed by absorption losses SE_A (-42 and -45dB) and partially by reflection losses SE_R (-12 and -11dB). In case CF- Fe_3O_4 -ZnO presence of ZnO nanoparticles along with ferrites nanoparticles improves the absorption losses. As reported in earlier section, ZnO nanoparticles is controlling agglomeration of Fe_3O_4 nanoparticles after coating on foam (CF- Fe_3O_4 -ZnO), which provide higher surface area and large interfacial area in comparison to CF-U and CF- Fe_3O_4 .

However, ZnO is dielectric material so addition of ZnO with Fe_3O_4 in carbon foam, influence electrical conductivity of carbon foam. Moreover reflection component is depend on electrical conductivity as shown in the following equation of SE of reflection component.

$$SE_R = -10 \log_{10} \left\{ \frac{\sigma_T}{16 \omega \epsilon_0 \mu'} \right\}$$

As a result ZnO is contribution in decreasing electrical conductivity as well as dielectric constant and as a consequence reduced in the magnetic properties. (Magnetization in Figure 7, is less of ZnO embedded with of Fe_3O_4 in carbon foam). So decreases the electrical conductivity of carbon foam decreases the reflection component of carbon foam resulting improved the absorption component.

To understand the possible mechanism in an improvement of absorption of EM radiation, EM parameters i.e., relative complex permittivity ($\epsilon^* = \epsilon' - i\epsilon''$) and relative complex permeability ($\mu^* = \mu' - i\mu''$) are measured in the frequency region 8.2-12.4 GHz of CFoams and depicted in **figure 6 (a-b)**. These obtained complex parameters have been estimated from experimental scattering parameters (S_{11} & S_{21}) by standard Nicholson-Ross and Weir theoretical calculation^{35, 36}. The estimated real part of the EM parameters (ϵ' , μ') is directly associated with the amount of polarization occurring in the material which symbolizes the storage ability of the electric and magnetic energy, while the imaginary part (ϵ'' , μ'') is signifies the dissipated electric and magnetic energy. The complex values of permittivity and permeability typically correspond to attenuation in a medium in which real permittivity and permeability is related to wave propagation rather than attenuation.

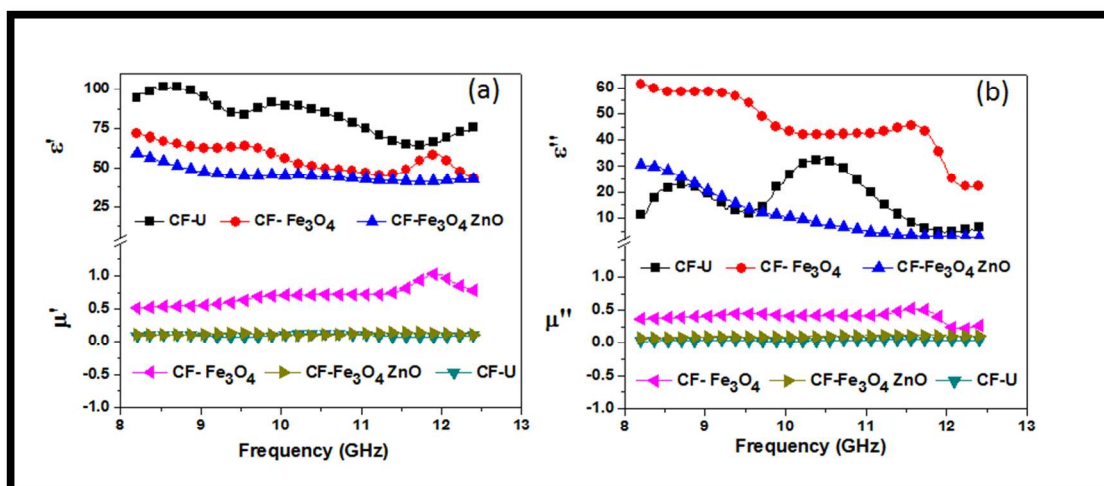


Figure 6: The complex permittivity and permeability of the CFoam

In this direction as reported above, effect of Fe₃O₄ and Fe₃O₄-ZnO coating on real permittivity and permeability depicted in figure 6 (a). The real permittivity in all the types of CFoams (CFU, CF-Fe₃O₄ and CF-Fe₃O₄-ZnO) decreases slightly with increasing the frequency and maximum value of permittivity is in case of CF-U and minimum in CF-Fe₃O₄ZnO. If compared the value of electrical conductivity and real permittivity, both are in concurrent with each other. The real part of complex permittivity is an expression of polarization ability of foam which mainly arises from dipolar polarization and interfacial polarization³⁷. In case of CF-U due to the higher value of conductivity, interfacial and dipole polarization contributes in its overall polarization capability³⁸. Whereas imaginary permittivity shows the opposite trend, imaginary permittivity is maximum in case of CF-Fe₃O₄ and minimum in case of CF-U which is related to losses. The decreasing the permittivity with frequency could be ascribed to the decreasing capacity of the dipoles to sustain the in phase movement with speedily pulsating electric vector of the incident radiation.

However, in case CF-Fe₃O₄ and CF-Fe₃O₄-ZnO due to the lower value of conductivity, interfacial polarization effect is comparatively small and as a result lowers value of real permittivity. Therefore, impedance is much closer to impedance of free space due to lower value of real permittivity and hence, minimizing reflectivity. Thus, it becomes highly capable of absorbing EM radiation rather than reflection. The higher the value of the imaginary component of

permittivity, larger is the loss in the material. A material with low dielectric loss can store energy, but will not dissipate the stored energy. The material with high dielectric loss does not store energy efficiently and larger part of the energy of the incident wave is converted into heat within the material. Therefore, materials with lower value of conductivity yield in to large amount of losses that inhibits the propagation of EM radiation i.e., absorption losses are more in case of CF-Fe₃O₄ and CF-Fe₃O₄-ZnO.

The ϵ'' of carbon foam CF-U varies with frequency and it is lower than the CF-Fe₃O₄-ZnO. The following equation SE-A is demonstrated that absorption component depends upon the magnetic permeability (μ') of the materials.

$$SE_A = -8.68t \{(\sigma_T \omega \mu')/2\}^{1/2}$$

The CFoam CF-U does not shows any magnetization and as a results CF-U shows the absorption component is minimum as compares to CF-Fe₃O₄-ZnO. The absorption loss not only depends upon only magnetic permeability but also conductivity and frequency. The material cannot always absorption dominated in the whole frequency range. But the value of ϵ'' should be less than ϵ' , this demonstrated in Figure 6 (a & b).

Thus, higher value of real permeability is also responsible for the radiation absorption. In CFoam, the existence of interfaces between Fe₃O₄ nanoparticles-CFoam, ZnO nanoparticles-CFoam, and Fe₃O₄-ZnO are responsible for interfacial polarization which further contribute in the dielectric losses. Interfacial polarization occurs in heterogeneous media due to accumulation of charges at the interfaces and the formation of large dipoles. Ferromagnetic nanoparticles act as tiny dipoles which get polarized in the presence of EM field and result in better microwave absorption.

The maximum real permeability is of Fe₃O₄ coated foam among all the CFoam. This is possibly due to the improvement of magnetic properties along the parallel reduction of eddy current losses due to the ferromagnetic behaviour of coating material. While real permeability is almost negligible in case of CF-U due to the nonmagnetic behaviour of CFoam. When the frequency of the applied field increases, magneto-crystalline anisotropy plays the important role³⁹ and induced magnetization start to delay behind the applied field resulting in the magnetic losses. The anisotropic effect is much stronger in

case Fe_3O_4 nanoparticles coated foam and as a consequence large difference between magnetization and applied field leading to enhanced magnetic losses. In the same fashion the imaginary permeability (magnetic loss) is vary with increasing the frequency. The Fe_3O_4 particle coating on CFoam also leads to matching input impedance along with reduction of skin depth which is also contribute towards absorption of EM radiations. In the microwave ranges, the natural resonances in the X-band can be attributed to the small size of Fe_3O_4 and ZnO nanoparticles in CFoams. Anisotropy energy of the small size materials, especially in the nanoscale, would be higher due to the surface anisotropic field due to the small size effect⁴⁰. The higher anisotropy energy also contributes in the enhancement of the microwave absorption. On the same pattern magnetic losses varies with frequency, in case of CF- Fe_3O_4 both real and imaginary part of complex permeability increases with frequency and it is maximum between 10 and 12 GHz while in CF-U and CF- Fe_3O_4 -ZnO it is constant with increasing the frequency. This has positive effect on absorption of microwave radiation. The magnetic and dielectric coating on the surface of the CFoam leads to better matching of input impedance along with the reduction of skin depth. This is attributing further in the increase in absorption losses of foam.

Figure 5 (d) shows total losses with increasing frequency which is associated with sum of both dielectric and magnetic losses. From the figure 5 (d), it is evident that maximum total losses are in case CF- Fe_3O_4 which is associated to the magnetic properties of Fe_3O_4 while in case of CF- Fe_3O_4 -ZnO it is associated with magnetic as well as dielectric losses. This clearly brings that total losses in case CF- Fe_3O_4 -ZnO are less than CF- Fe_3O_4 , this reveals that magnetic losses are dominating in improvement of SE due to the more contribution of ferromagnetic material. This shows that SE is highly dominated by magnetic losses. This fact is verified by measuring magnetic properties by VSM.

Figure 7 shows the room temperature magnetization plot of CFoams CFU, CF- Fe_3O_4 and CF- Fe_3O_4 -ZnO. The data of magnetization reveals that CFU does not show any magnetization though out the magnetic field because carbon is in the amorphous phase with high electrical conductivity due to delocalized π electron. However, Fe_3O_4 and Fe_3O_4 -ZnO coated CFoam display narrow hysteresis loop. The CF- Fe_3O_4 possesses saturation magnetization 4.68 emu/g at

4.9 KG and CF-Fe₃O₄-ZnO possesses saturation magnetization 3.36 emu/g. The higher saturation magnetization in case of CF-Fe₃O₄ is due to the magnetic properties of Fe₃O₄. These results are in the agreement with data of magnetic permeability and shielding effectiveness.

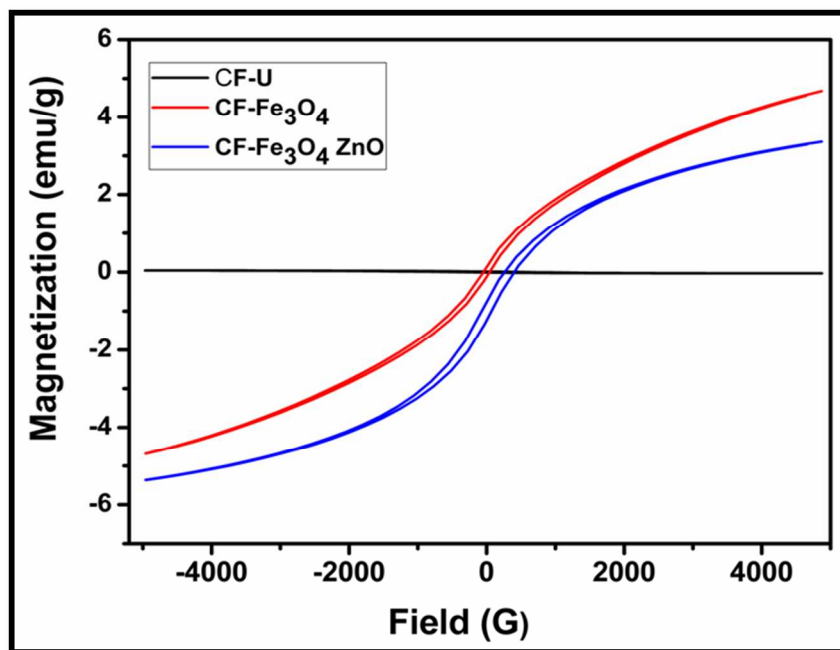


Figure 7: Magnetization plot of CFoams CFU, CF-Fe₃O₄ and CF-Fe₃O₄-ZnO

Thermal stability of the CFoam is investigated by TGA in oxidative (air) atmosphere is depicted in **figure 8**. The thermal stability of CFoam is depend on structure of carbon, graphitic structure possess higher thermal stability as compared non graphitic carbon⁴¹. It is observed that, coated CFoam (CF-Fe₃O₄ and CF-Fe₃O₄-ZnO) possess higher thermal stability as compared to CF-U. The coating of Fe₃O₄ and ZnO enhances the thermal stability of CFoam by ~100°C. In case of CF-U, weight loss initiated from temperature ~500°C and total weight loss take place up to 650°C. While in case CF-Fe₃O₄ and CF-Fe₃O₄-ZnO weight loss is initiated from 600°C. In an oxidizing environment, weight loss initiation takes place from chemically active site available in 1000°C heat treated CFoam which reacts with oxygen molecule. On the other hand in case CF-Fe₃O₄ and CF-Fe₃O₄-ZnO, the coating of nano Fe₃O₄ and ZnO make interaction with chemically active site during the heat treatment. This is responsible in the improvement of thermal stability of the CF-Fe₃O₄ and CF-Fe₃O₄-ZnO foams.

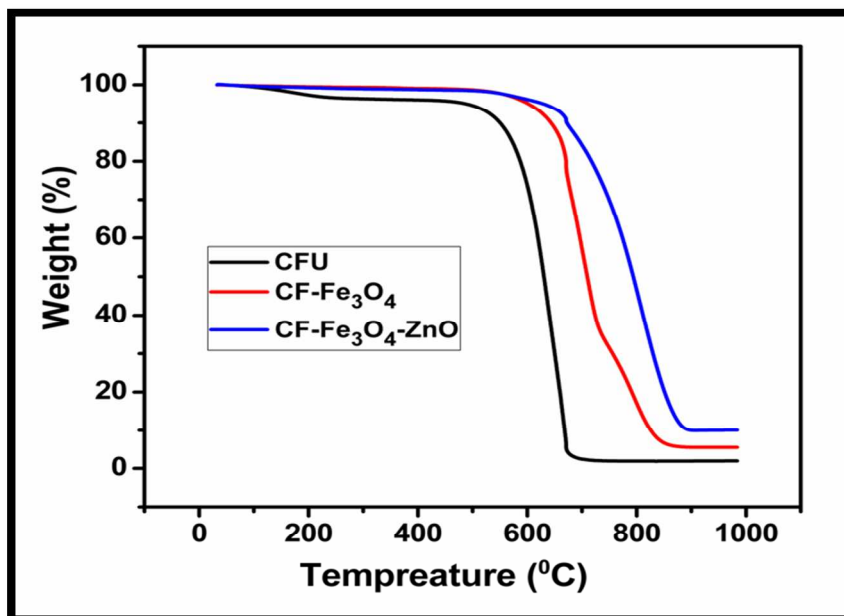


Figure 8: Thermal stability of CFoam in oxidative (air) atmosphere

4. Conclusions

The CFoam developed by sacrificial template technique using coal tar pitch as carbon precursor and it is decorated by Fe_3O_4 and $\text{Fe}_3\text{O}_4\text{-ZnO}$ nanoparticles to improve electromagnetic radiation absorption. It is observed that, small uptake (10% enhancement in density) of magnetic and dielectric nanoparticles coating on the conducting CFoam significantly influence the EM radiation scattering. The nanoparticles coating not only improved the EM radiation absorption but also enhanced compressive strength and thermal stability of CFoam. The CFoam total SE is in the range of -25 dB which increases to -54 and -56 dB after Fe_3O_4 and $\text{Fe}_3\text{O}_4\text{-ZnO}$ nanoparticles coating. But the enhancement in SE is due to the absorption losses and which is contributed by -42 and -45dB. The EM radiation absorption enhancements in case of Fe_3O_4 and $\text{Fe}_3\text{O}_4\text{-ZnO}$ decorated CFoam are mainly from the magnetic losses which is verified from the data of complex permittivity and permeability, and magnetic properties measured by vibration sample magnetometer. The maximum complex permittivity and magnetization is in case of Fe_3O_4 coated CFoam as compared to other. This shows that the improvement of absorption of EM radiation is mostly due to the magnetic losses. The Thermogravimetric study reveals that Fe_3O_4 and $\text{Fe}_3\text{O}_4\text{-ZnO}$ coating improves the thermal stability of CFoam by 100°C. This

clearly demonstrate that small uptake of Fe_3O_4 and Fe_3O_4 -ZnO nanoparticles coating on conducting CFoam is significantly useful to make it as RAM for sheath technology applications.

Acknowledgments

Authors are highly grateful to Director, CSIR-NPL, for his kind permission to publish the results. Authors are like to thanks Dr. S.K. Dhawan, Polymeric & Soft Materials Section for measurement of EMI shielding. The authors are thankful to Dr. R.K. Kotnala for magnetic properties measurement and Dr. R.P. Pant, for providing ferrofluid suspension. Also, acknowledge to Mr. Jai Tawale for providing help in SEM characterization.

References

1. M. S. Pinho, M. L. Gregori, R. C. R. Nunes and B. G. Soares, *European Polymer Journal*, 2002, 38, 2321-2327.
2. I. S. Seo, W. S. Chin and D. G. Lee, *Composite Structures*, 2004, 66, 533-542.
3. K.-Y. Park, S.-E. Lee, C.-G. Kim and J.-H. Han, *Composites Science and Technology*, 2006, 66, 576-584.
4. J.-H. Oh, K.-S. Oh, C.-G. Kim and C.-S. Hong, *Composites Part B: Engineering*, 2004, 35, 49-56.
5. R. A. Stonier, *Sampe Journal*, 1991, 27, 9-17.
6. J. Klett, A. McMillan, N. Gallego and C. Walls, *Journal of materials science*, 2004, 39, 3659-3676.
7. M. Inagaki, T. Morishita, A. Kuno, T. Kito, M. Hirano, T. Suwa and K. Kusakawa, *Carbon*, 2004, 42, 497-502.
8. F. C. Cowlard and J. C. Lewis, *Journal of materials science*, 1967, 2, 507-512.
9. C. Chen, E. B. Kennel, A. H. Stiller, P. G. Stansberry and J. W. Zondlo, *Carbon*, 2006, 44, 1535-1543.
10. M.-x. Wang, C.-Y. Wang, T.-Q. Li and Z.-J. Hu, *Carbon*, 2008, 46, 84-91.
11. T. Noda, M. Inagaki and S. Yamada, *Journal of Non-Crystalline Solids*, 1969, 1, 285-302.
12. R. Klett, *High temperature insulating carbonaceous material*, 1975.
13. R. Luo, Y. Ni, J. Li, C. Yang and S. Wang, *Materials Science and Engineering: A*, 2011, 528, 2023-2027.
14. S. Wang, R. Luo and Y. Ni, *Materials Science and Engineering: A*, 2010, 527, 3392-3395.
15. J. Klett, R. Hardy, E. Romine, C. Walls and T. Burchell, *Carbon*, 2000, 38, 953-973.
16. J. W. Klett, A. D. McMillan, N. C. Gallego, T. D. Burchell and C. A. Walls, *Carbon*, 2004, 42, 1849-1852.
17. Y. Chen, B.-Z. Chen, X.-C. Shi, H. Xu, Y.-J. Hu, Y. Yuan and N.-B. Shen, *Carbon*, 2007, 45, 2132-2134.
18. R. Kumar, S. R. Dhakate and R. B. Mathur, *Journal of materials science*, 2013.
19. R. Kumar, S. R. Dhakate, P. Saini and R. B. Mathur, *RSC Advances*, 2013.
20. R. Kumar, S. R. Dhakate, T. Gupta, P. Saini, B. P. Singh and R. B. Mathur, *J. Mater. Chem. A*, 2013, 1, 5727-5735.

21. M. Saitoh, T. Yamamoto, T. Sakamoto, H. Niori, M. Chino and M. Kobayashi, *Ferroelectrics*, 2001, 263, 9-12.
22. J. L. Kirschvink, *Bioelectromagnetics*, 1996, 17, 187-194.
23. D. K. Kim, M. S. Amin, S. Elborai, S.-H. Lee, Y. Koseoglu, M. Zahn and M. Muhammed, *Journal of applied physics*, 2005, 97, 10J510.
24. A. Yadav, R. Kumar, G. Bhatia and G. Verma, *Carbon*, 2011, 49, 3622-3630.
25. B. Wang, Q. Wei and S. Qu, *Int. J. Electrochem. Sci*, 2013, 8, 3786-3793.
26. H. El Ghandoor, H. Zidan, M. M. Khalil and M. Ismail, *Int. J. Electrochem. Sci*, 2012, 7, 5734-5745.
27. S. Y. Bae, C. W. Na, J. H. Kang and J. Park, *The Journal of Physical Chemistry B*, 2005, 109, 2526-2531.
28. H. Itoh and T. Sugimoto, *Journal of colloid and interface science*, 2003, 265, 283-295.
29. J. Yang, X. Liu, L. Yang, Y. Wang, Y. Zhang, J. Lang, M. Gao and M. Wei, *Journal of Alloys and Compounds*, 2009, 485, 743-746.
30. A. K. Zak, M. E. Abrishami, W. Majid, R. Yousefi and S. Hosseini, *Ceramics International*, 2011, 37, 393-398.
31. W. Wu, Z. Zhu, Z. Liu, Y. Xie, J. Zhang and T. Hu, *Carbon*, 2003, 41, 317-321.
32. S. Dhakate and O. Bahl, *Carbon*, 2003, 41, 1193-1203.
33. Y. Yang, M. C. Gupta, K. L. Dudley and R. W. Lawrence, *Advanced Materials*, 2005, 17, 1999-2003.
34. X. Han and Y. Wang, *JOURNAL OF FUNCTIONAL MATERIALS AND DEVICES*, 2007, 13, 529.
35. A. Nicolson and G. Ross, *Instrumentation and Measurement, IEEE Transactions on*, 1970, 19, 377-382.
36. A. P. Singh, P. Garg, F. Alam, K. Singh, R. Mathur, R. Tandon, A. Chandra and S. Dhawan, *Carbon*, 2012, 50, 3868-3875.
37. G. Burns, Academic Press, New York.
38. S. J. Penn, N. M. Alford, A. Templeton, X. Wang, M. Xu, M. Reece and K. Schrapel, *Journal of the American Ceramic Society*, 1997, 80, 1885-1888.
39. D. Dimitrov and G. Wysin, *Physical Review B*, 1995, 51, 11947.
40. A. P. Singh, M. Mishra, P. Sambyal, B. K. Gupta, B. P. Singh, A. Chandra and S. K. Dhawan, *Journal of Materials Chemistry A*, 2014, 2, 3581-3593.
41. S. Dhakate, P. Bahl and P. Sahare, *Journal of materials science letters*, 2000, 19, 1959-1961.